IEEE Access
Multidisciplinary ⋮ Rapid Review ⋮ Open Access Journal

Received April 27, 2019, accepted May 15, 2019, date of publication May 17, 2019, date of current version June 3, 2019.

Digital Object Identifier 10.1109/ACCESS.2019.2917587

On the Discretized Gaussian Modulation (DGM)-Based Continuous Variable-QKD

IVAN B. DJORDJEVIC, (Senior Member, IEEE)
Department of Electrical and Computer Engineering, University of Arizona, Tucson, AZ 85721, USA
e-mail: ivan@email.arizona.edu

This work was supported by the ONR MURI program under Grant N00014-13-1-0627.

ABSTRACT To overcome the low reconciliation efficiency problem of Gaussian modulation (GM)-based-continuous variable (CV)-quantum key distribution (QKD), in this paper, we propose to use discretized GM (DGM)-based-CV-QKD. The proposed CV-QKD scheme has complexity and reconciliation efficiency similar to that of discrete modulation (DM)-based-CV-QKD and at the same time solves for the problem of the nonexistence of strict security proofs for the DM-CV-QKD under the collective attacks. We demonstrate that the 32-points-based DGM CV-QKD can closely approach the theoretical SKR-limit in medium and high channel losses regimes. On the other hand, the 64-points-based DGM CV-QKD scheme closely approaches the SKR-limit for all channel losses.

INDEX TERMS Quantum communication, quantum key distribution (QKD), continuous variable (CV)-QKD, Gaussian modulation, discrete modulation, information reconciliation, secret-key rate (SKR).

I. INTRODUCTION

Thanks to the recent satellite-to-ground QKD demonstration [1], the research in QKD is getting momentum. Discrete variable (DV)-QKD schemes achieve unconditional security by employing no-cloning theorem. On the other hand, continuous variable (CV)-QKD schemes employ the uncertainty principle. One of the key limitations for DV-QKD represents long deadtime of the single-photon detectors (SPDs), which limits the baud rate and therefore the secret-key rate (SKR). In contrast, the CV-QKD schemes employ the homodyne/heterodyne detection instead and as such do not exhibit this problem. Very popular CV-QKD protocols are those based on either discrete modulation (DM) [2]–[6] or Gaussian modulation (GM) [7], [8]. One of the key disadvantages of GM is related to its low reconciliation efficiency [7], [8]. The DM-based CV-QKD protocols, instead, have much better information reconciliation (error correction) efficiency and are compatible with state-of-the-art fiber-optics communications' equipment. Unfortunately, strict security proofs of DM-based CV-QKD for collective attacks are still not well developed.

To overcome these key challenges for DV-QKD as well as for DM-based CV-QKD, such as a nonexistence of accurate security proofs, we propose to employ discretized GM (DGM)-based CV-QKD protocol. The proposed QKD scheme employs the Gaussian source implemented in electrical domain instead of the optical Gaussian source. This scheme has complexity and reconciliation efficiency comparable to that of DM-CV-QKD schemes and solves for the strict unconditional security problem of DM-CV-QKD under collective attacks. We demonstrate that for all transmission losses the 32-points generated from Gaussian source in digital-domain in time-varying fashion are sufficient to closely approach theoretical SKR-limit. We also show that signal constellations designed to faithfully represent the Gaussian source can also closely approach the SKR-limit, when used in time-varying fashion.

The paper is organized as follows. The conventional GM-based CV-QKD scheme is described in Section II. In Section III, the proposed discretized Gaussian modulation-based RF-assisted CV-QKD scheme is described. Details of the generalized RF-assisted heterodyne detector are provided in Section IV. The illustrative secret-key rate results are provided in Section V. Section VI provides some relevant concluding remarks.

II. CONVENTIONAL GAUSSIAN MODULATION-BASED CV-QKD SCHEMES

The CV-QKD can be implemented by employing either homodyne detection, where only one quadrature component is measured at a time (because of the uncertainty principle), or with heterodyne detection (HD), where one beam splitter (BS) and two balanced photodetectors are used

The associate editor coordinating the review of this manuscript and approving it for publication was Jiafeng Xie.

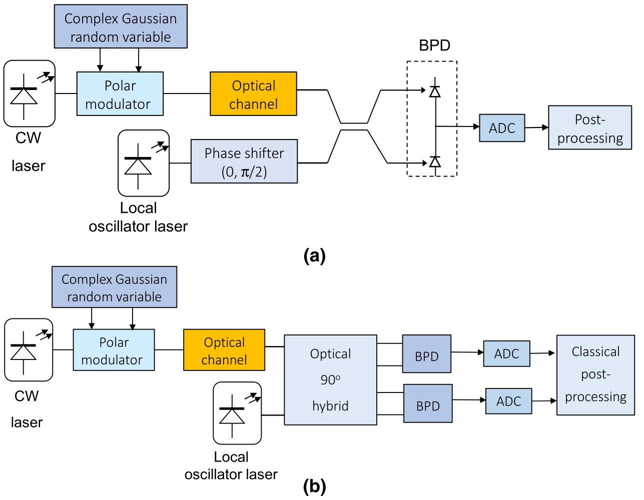

FIGURE 1. Illustrating Gaussian modulation-based CV-QKD protocols: (a) homodyne detection-based CV-QKD scheme, and (b) heterodyne detection-based CV-QKD scheme. ADC: Analog-to-digital conversion, BPD: Balanced photodetection.

to measure both quadrature components simultaneously, as illustrated in Fig. 1. To impose the Gaussian modulation on coherent optical state, instead of optical-domain, we propose to use the electrical-domain instead (see Fig. 1). For this purpose, we can use either polar coordinates (ρ,ϕ) or Cartesian coordinates (I,Q). In polar coordinates, the 2-D modulator is composed of a cascade of an amplitude modulator and a phase modulator. When the RF input to the amplitude modulator follows the Rayleigh distribution, while the phase is uniform, resulting 2-D distribution will be complex Gaussian. HD can double the mutual information between Alice and Bob compared to the homodyne detection scheme at the expense of additional 3 dB loss of the beam splitter (BS). In order to reduce the laser phase noise, the quantum signals are typically co-propagated together with the time-domain multiplexed high-power pilot-tone (PT) to align Alice's and Bob's measurement bases. To implement CV-QKD both squeezed states and coherent states can be employed.

Squeezed states-based protocols employ the Heisenberg uncertainty principle, claiming that it is impossible to measure both quadratures with arbitrary precision. To impose the information, Alice randomly selects to use either in-phase or quadrature degree of freedom (DOF). When in-phase DOF is used (encoding rule I), the squeezed state is imposed on the in-phase component (with squeezed parameter $s_I < 1$). On the other hand, in Alice encoding rule Q (when the quadrature is used), the squeezed state is imposed on the quadrature (with squeezed parameter $s_Q > 1$). On the receiver side, Bob randomly selects whether to measure either in-phase component or quadrature component. Alice and Bob exchange the encoding rules being used by them to measure the quadrature for every squeezed state and keep only instances when they measured the same quadrature in the sifting procedure. Therefore, this protocol is very similar to the BB84 protocol. After that the information reconciliation takes place, followed by the privacy amplification.

In coherent state-based protocols, there is only one encoding rule for Alice. Alice randomly selects a point in 2-D (I,Q) space from a zero-mean circular symmetric Gaussian distribution. Clearly, both quadratures have the same uncertainty. Here we again employ the Heisenberg uncertainty principle. On receiver, side Bob performs the random measurement on either in-phase or quadrature component. When Bob measures the in-phase component, his measurement is correlated with the in-phase coordinate of signal constellation point sent by Alice. On the other hand, when Bob measures the quadrature component, his measurement result is correlated with Alice's quadrature coordinate of transmitted signal constellation point. Clearly, with homodyne detection, Bob is able to measure a single coordinate of the signal constellation point sent by Alice using Gaussian coherent state. Bob then announces which quadrature he measured in each signaling interval, and Alice selects the coordinate that agrees with Bob's measurement quadrature. The rest of the protocol is the same as for the squeezed states-based protocol.

The CV-QKD system experience the 3 dB loss limitation in transmittance when the direct reconciliation is used. To avoid for this problem either reverse reconciliation [10] or the postelection [11] methods are used. It has been shown that for Gaussian modulation, Gaussian attack is an optimum attack for both individual attacks [12] and collective attacks [13], [14]. In incoming section, we described our proposed discretized GM-based CV-QKD scheme, which can closely approach the theoretical SKR-limit.

III. PROPOSED DISCRETIZED GAUSSIAN MODULATION (DGM)-BASED CV-QKD SCHEME

To initialize the proposed QKD system, Alice and Bob preshare the common sequence of seeds, corresponding to different sizes M of signal constellations generated from Gaussian source, to be used in subsequent discretized GM-DV-QKD. In initialization stage, Alice selects at random seed to be used for Gaussian noise generator. She then generates at random a sequence of points from Gaussian random generator. She then splits this sequence into subsequences of length M. In transmission stage, Alice further randomly selects the subsequence (Gaussian signal constellation) to use, followed by a random selection of point from that subsequence, and imposes it on an RF subcarrier. In-phase and quadrature components of such generated points, with the help of arbitrary waveform generator (AWG), are used as RF inputs of an electro-optical (EO) I/Q modulator, as shown in Fig. 2. After the adjustment of the variance v_A by the variable optical attenuator (VOA), such obtained pulse is sent to Bob over the quantum channel. The channel is characterized by transmissivity T and excess noise ε so that total channel added noise variance, referred to the channel input, can be expressed in shot-noise unit (SNU) by $\chi_{\text{line}} = 1/T - 1 + \varepsilon$.

On receiver side, Bob employs the heterodyne coherent detection together with a phase-noise cancellation (PNC) stage [2], [3] to control the level of excess noise. The PNC stage first squares the reconstructed in-phase and quadrature

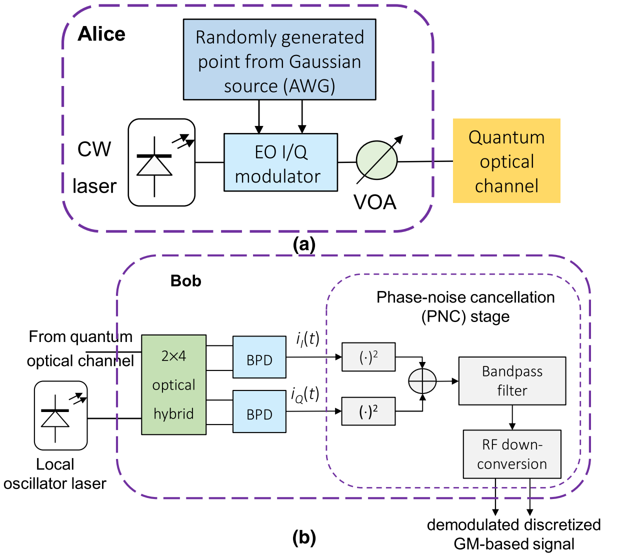

FIGURE 2. **The proposed RF-assisted discretized GM-CV-QKD scheme. The configurations of: (a) Alice's transmitter and (b) Bob's receiver. VOA: Variable optical attenuator, BPD: Balanced photodetector.**

signals and after that either adds or subtracts them depending on the optical hybrid type [16]. The PNC stage further performs bandpass filtering to remove DC component and double-frequency terms, followed by the down-conversion, implemented with the help of multipliers and low-pass filters. On such a way Bob detects a point out of M possible points from the subsequence, in similar fashion as for DM. Given that PNC stage cancels the phase noise and frequency offset fluctuations, it exhibits better tolerance to the excess noise compared to the traditional DM-based CV-QKD schemes. Additional details on the generalized RF-assisted heterodyne detection scheme can be found in Sec. IV.

In sifting procedure, Alice announces the indices of the seeds being used in every signaling interval. Given that Bob knows the seeds he can easily identify Gaussian signal constellation being used. After that Alice and Bob perform conventional parameter estimation and classical postprocessing (information reconciliation and privacy amplification) steps. Clearly, the receiver complexity is comparable to DM QKD schemes, but the proposed scheme preserves the unconditional security under collective attacks offered by GM-based QKD scheme.

IV. DESCRIPTION OF GENERALIZED RF-ASSISTED HETERODYNE DETECTION SCHEME

The generic RF-assisted CV-QKD scheme described here is applicable to any two-dimensional (2-D) signal constellation and as such it represents a generalization of scheme presented in [3], which considers only M-PSK signals. The in-phase and quadrature components 2-D constellation point imposed on RF-subcarrier can be represented as:

$$\begin{aligned} s_I(t) &= A\mathrm{Re}\left\{(I(t)+jQ(t))\,e^{j\omega_{RF}t}\right\} \\ &= A\left[I(t)\cos(\omega_{RF}t) - Q(t)\sin(\omega_{RF}t)\right], \end{aligned} \tag{1a}$$

$$\begin{aligned} s_Q(t) &= A\mathrm{Im}\left\{(I(t)+jQ(t))\,e^{j\omega_{RF}t}\right\} \\ &= A\left[Q(t)\cos(\omega_{RF}t) + I(t)\sin(\omega_{RF}t)\right], \end{aligned} \tag{1b}$$

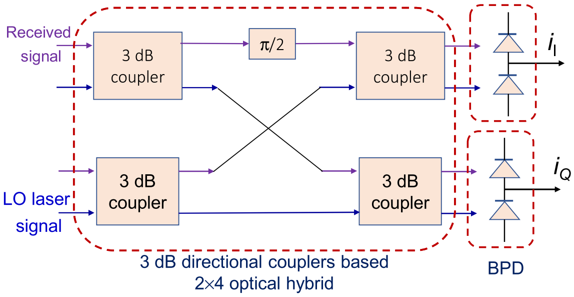

FIGURE 3. **The configuration of 2 × 4 optical hybrid used in Fig. 2, based on 3dB directional couplers, followed by balanced photodetectors (BPDs).**

where ω_{RF} is the RF radial frequency [rad/s], while $I(t)$ and $Q(t)$ represent the in-phase and quadrature coordinates of the RF signal. The modulation constant A is used to vary the modulation variance of the signal v_{A}, typically expressed in SNU. For instance, for 8-star-QAM we have that $(I, Q) \in\{(1,1), (-1,1), (-1,-1), (1, -1), (1+\sqrt{3},0), (0, 1+\sqrt{3}), (-1-\sqrt{3},0), (0,-1-\sqrt{3})\}$. The RF-subcarrier signal can be generated with the help of an arbitrary waveform generator (AWG). Alternatively, an RF mixer can be used instead. By biasing both in-phase and quadrature branches of the EO I/Q modulator at $\pi/4$-point, which is achieved by setting the DC voltage to $V_\pi/4$ (where the V_π is the half-wave switching voltage), the in-phase RF input of I/Q modulator can be written as $V_I(t) = (2/\pi)V_\pi s_I(t)$, while the quadrature RF input by $V_Q(t) = (2/\pi)V_\pi s_Q(t)$, so that the I/Q modulator output signal can be represented (in small signal analysis) as:

$$\begin{aligned} E_o(t) \cong{}& \sqrt{\frac{P_s}{2}}e^{j(\omega_{Tx}t+\phi_{Tx}+\pi/4)} \\ &- A\left[I(t)+jQ(t)\right]\sqrt{P_s}e^{j[(\omega_{Tx}+\omega_{RF})t+\phi_{Tx}]}. \end{aligned} \tag{2}$$

In Eqn. (2), P_s denotes the laser output power, ω_{Tx} is the transmit laser radial frequency, and ϕ_{Tx} represents the transmit laser phase noise process. Therefore, the first term represents unmodulated optical carrier, while the second term represents the modulated signal.

On receiver side, when 2×4 optical hybrid, based on 3dB directional couplers, is used as shown in Fig. 3, by squaring and subtracting the in-phase and quadrature photocurrents, denoted respectively as i_I and i_Q, followed by bandpass filtering (BPF) to remove the DC component and double-frequency terms, we obtain:

$$\begin{aligned} r(t) &= \frac{1}{R^2 P_s P_{LO}\sqrt{2}}BPF\left[i_I^2(t) - i_Q^2(t)\right] \\ &= A\left[I(t)\cos(\omega_{RF}t-\pi/4) - Q(t)\sin(\omega_{RF}t-\pi/4)\right] \\ &\quad + n_{NB}(t), \end{aligned} \tag{3}$$

where $n_{\mathrm{NB}}(t)$ denotes the equivalent narrowband noise at RF subcarrier level, P_{LO} denotes the power of local oscillator laser, and R denotes the photodiode responsivity. Now we perform the down-conversion process [multiplication followed by the low-pass filters (LPFs)] to obtain:

$$r_I(t) \cong LPF\left[r(t)\,2\cos\left(\omega_{RF}t-\pi/4\right)\right] \cong AI(t)+n'_I,$$
$$r_Q(t) \cong LPF\left[r(t)\,2\sin\left(\omega_{RF}t-\pi/4\right)\right] \cong -AQ(t)+n'_Q, \quad (4)$$

where n'_{I} and n'_{Q} are equivalent in-phase and quadrature low-pass additive noise processes. Clearly, the outputs of down-conversion block are proportional to in-phase and quadrature components of transmitted signal. Even though this scheme is described in context of 2-D modulation schemes, such as M-ary PSK and M-ary QAM, this scheme is also applicable to any higher-dimensional signaling schemes.

V. ILLUSTRATIVE SKR RESULTS

The expression for secret fraction (SF), obtained by one-way postprocessing, for reverse reconciliation, is given by:

$$SF = \beta I(A;B) - \chi(B;E), \quad (5)$$

where $I(A;B)$ represents the mutual information between Alice and Bob, while the second term $\chi(B;E)$ corresponds to the Holevo information between Eve and Bob. We use β to denote the reconciliation efficiency. For the GM with heterodyne detection the mutual information is calculated by:

$$I(A;B) = \log_2\left(\frac{v+\chi_{\mathrm{total}}}{1+\chi_{\mathrm{total}}}\right), \quad (6)$$

where $\chi_{\mathrm{total}} = \chi_{\mathrm{line}} + \chi_{\mathrm{het}}/T$ with χ_{het} representing the variance due to heterodyne detection being equal to $[1 + (1-\eta) + 2v_{\mathrm{el}}]/\eta$, with η denoting the detector efficiency. In Eqn. (6), $v = v_A + 1$, with v_A being the average Alice's variance. However, for the discretized Gaussian modulation with subsequences of size M, the expression (6) is not applicable. The mutual information $I(A;B)$ for DGM is calculated as described in [17], [18]; in other words, we can write:

$$I(A;B) = \log_2 M - E_{\mathbf{z}}\left\{\frac{1}{M}\sum_{m=0}^{M-1}\log_2\sum_{k=0}^{M-1} e^{-\frac{\left(s_{k,I}+z_I-s_{m,I}\right)^2+\left(s_{k,Q}+z_Q-s_{m,Q}\right)^2}{2\sigma^2}}\right\}, \quad (7)$$

where $\boldsymbol{s}_m = (s_{m,\mathrm{I}}, s_{m,\mathrm{Q}})$ is the transmitted symbol, $\boldsymbol{s}_k$ is a possible received symbol, and σ^2 is the variance of Gaussian channel noise. Clearly, the expectation operator E{·} is applied for different additive complex Gaussian noise realizations, that is z=$[z_1 z_2 \ldots z_l \ldots]^{\mathrm{T}}$, where $z_l = z_{l,\mathrm{I}}$+j$z_{l,\mathrm{Q}}$.

The Holevo information between Bob and Eve, for heterodyne detection, is determined by [7]–[15]:

$$\chi(B;E) = g\left(\frac{\lambda_1-1}{2}\right)+g\left(\frac{\lambda_2-1}{2}\right) - g\left(\frac{\lambda_3-1}{2}\right)-g\left(\frac{\lambda_4-1}{2}\right), \quad (8)$$

where $g(x) = (x+1)\log_2(x+1) - x\log_2 x$ is the entropy of a thermal state with the mean number of photons being x.

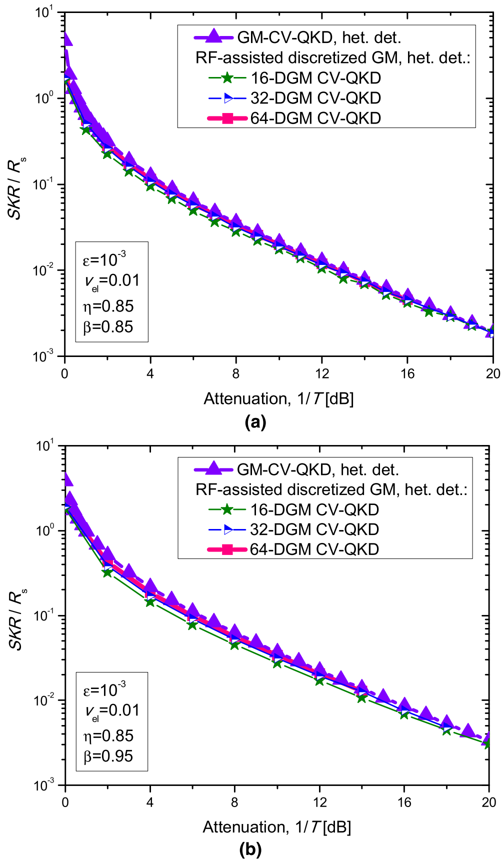

FIGURE 4. **Normalized SKRs for proposed discretized GM-QKD protocol vs. channel loss for different signal constellation sizes assuming that reconciliation efficiency is: (a) $\beta = 0.85$ and (b) $\beta = 0.95$.**

The λ-parameters are defined by [7]–[15]:

$$\lambda_{1,2} = \sqrt{\frac{1}{2}\left(A\pm\sqrt{A^2–4B}\right)}, \quad \lambda_{3,4} = \sqrt{\frac{1}{2}\left(C\pm\sqrt{C^2–4D}\right)}, \quad (9)$$

where A, B, C, and D parameters are determined by [7]–[15]:

$$A = v^2(1–2T)+2T+T^2(v+\chi_{\mathrm{line}})^2, \quad B = T^2(1+Tv\chi_{\mathrm{line}})^2,$$
$$C = \frac{A\chi_{het}^2+B+1+2\chi_{het}\left[v\sqrt{B}+T(v+\chi_{\mathrm{line}})\right]+2T\left(v^2-1\right)}{T^2(v+\chi_{\mathrm{total}})^2},$$
$$D = \frac{\left(v+\chi_{\mathrm{het}}\sqrt{B}\right)^2}{T^2(v+\chi_{\mathrm{total}})^2}. \quad (10)$$

For CV-QKD schemes, the secrecy rate can be interpreted as the normalized SKR, where the normalization is with respect to the signaling rate R_{s}.

In Fig. 4, we provide the SKR results for the proposed DGM-based CV-QKD protocol, for different subsequences (constellation) sizes.

In calculations, the electrical noise variance is set to $v_{\mathrm{el}} = 10^{-2}$, the excess noise variance to $\varepsilon = 10^{-3}$, detector efficiency is set to $\eta = 0.85$, and reconciliation efficiency is

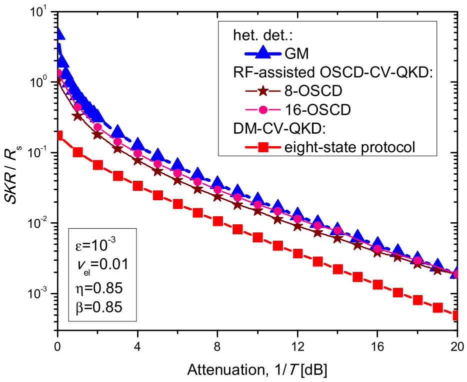

FIGURE 5. Normalized SKRs when OSCD-based CV-QKD is used for different signal constellation sizes.

set to $\beta = 0.85$ in Fig. 4(a) and $\beta = 0.95$ in Fig. 4(b). Clearly, for channel loss larger than 18 dB, discretized GM with 16 points is sufficient to achieve the theoretical GM-CV-QKD limit. For smaller channel loss values there is a certain degradation in normalized SKR. On the other hand, the discretized-GM with 32 points closely approaches the SKR-limit for both medium and high channel losses. Finally, the discretized GM-based CV-QKD with 64 points closely approaches the theoretical SKR-limit for all channel loss, except when channel loss is close to 0 dB.

We also study the SKR performance of a particular version of discretized GM-QKD, in which for each seed the optimized signal constellation design (OSCD) algorithm [19] is run based on a training sequence from the Gaussian generator to get faithful representation of the source. In this version, the coordinates of corresponding OSCD constellations are stored in look-up-table (LUT). The index of the seed is now used as an address to get the coordinates from the LUT. The SKR results are summarized in Fig. 5, for the same parameters being used in Fig. 4(a). For channel loss larger than 18 dB, the 8-OSCD-based QKD scheme closely approaches theoretical GM-QKD SKR-limit. On the other hand, 16-OSCD-based CV-QKD scheme closely approaches the SKR-limit for channel losses larger than 12 dB. For comparison purposes, the SKR results for eight-state DM-CV-QKD protocol, proposed in [6], are provided as well, which are well below the 8-OSCD-based CV-QKD scheme.

VI. CONCLUDING REMARKS

To solve for low reconciliation efficiency problem of the GM-based CV-QKD scheme, we have proposed to use the discretized GM-based CV-QKD. This scheme has complexity and reconciliation efficiency similar to the DM-based CV-QKD and at the same time solves for the problem of nonexistence of strict security proofs for DM-based CV-QKD schemes under collective attacks. In medium and high transmission loss regimes 32-DGM-based CV-QKD scheme closely approaches the theoretical SKR-limit. On the other hand, 64-DGM-based scheme approaches the SKR-limit for all attenuation regimes. The 16-OSCD-based CV-QKD scheme closely approaches SKR-limit for channel loss larger than 12 dB.

REFERENCES

[1] S.-K. Liao *et al.*, "Satellite-to-ground quantum key distribution," *Nature*, vol. 549, no. 7670, pp. 43–47, Sep. 2017.
[2] Z. Qu and I. B. Djordjevic, "Four-dimensionally multiplexed eight-state continuous-variable quantum key distribution over turbulent channels," *IEEE Photon. J.*, vol. 9, no. 6, Dec. 2017, Art. no. 7600408.
[3] Z. Qu, I. B. Djordjevic, and M. A. Neifeld, "RF-subcarrier-assisted four-state continuous-variable QKD based on coherent detection," *Opt. Lett.*, vol. 41, no. 23, pp. 5507–5510, Dec. 2016.
[4] T. C. Ralph, "Continuous variable quantum cryptography," *Phys. Rev. A, Gen. Phys.*, vol. 61, Dec. 1999, Art. no. 010303.
[5] R. Namiki and T. Hirano, "Security of quantum cryptography using balanced homodyne detection," *Phys. Rev. A, Gen. Phys.*, vol. 67, Feb. 2003, Art. no. 022308.
[6] A. Becir, F. A. A. El-Orany, and M. R. B. Wahiddin, "Continuous-variable quantum key distribution protocols with eight-state discrete modulation," *Int. J. Quantum Inform.*, vol. 10, no. 1, Feb. 2012, Art. no. 1250004.
[7] R. S. García-Patrón, "Quantum information with optical continuous variables: From bell tests to key distribution," M.S. Thesis, Faculte des Sci. Appl. Theorie l'Inf. Commun., Université Libre de Bruxelles, Brussels, Belgium, 2007.
[8] C. Weedbrook *et al.*, "Gaussian quantum information," *Rev. Mod. Phys.*, vol. 84, no. 2, p. 621, May 2012.
[9] S. Fossier, E. Diamanti, T. Debuisschert, R. Tualle-Brouri, and P. Grangier, "Journal of physics B: Atomic, molecular and optical physics improvement of continuous-variable quantum key distribution systems by using optical preamplifiers," *J. Phys. B, At. Mol. Opt. Phys.*, vol. 42, May 2009, Art. no. 114014.
[10] F. Grosshans and P. Grangier. (2002). "Reverse reconciliation protocols for quantum cryptography with continuous variables." [Online]. Available: https://arxiv.org/abs/quant-ph/0204127
[11] C. Silberhorn, T. C. Ralph, N. Lütkenhaus, and G. Leuchs, "Continuous variable quantum cryptography: Beating the 3 dB Loss Limit," *Phys. Rev. Lett.*, vol. 89, Sep. 2002, Art. no. 167901.
[12] F. Grosshans and N. J. Cerf, "Continuous-variable quantum cryptography is secure against non-Gaussian attacks," *Phys. Rev. Lett.*, vol. 92, Jan. 2004, Arty. no. 047905.
[13] R. García-Patrón and N. J. Cerf, "Unconditional optimality of Gaussian attacks against continuous-variable quantum key distribution," *Phys. Rev. Lett.*, vol. 97, Nov. 2006, Art. no. 190503.
[14] M. Navascués, F. Grosshans, and A. Acín, "Optimality of Gaussian attacks in continuous-variable quantum cryptography," *Phys. Rev. Lett.*, vol. 97, Nov. 2006, Art. no. 190502.
[15] Y. Shen, H. Zou, L. Tian, P. Chen, and J. Yuan, "Experimental study on discretely modulated continuous-variable quantum key distribution," *Phys. Rev. A*, vol. 82, Aug. 2010, Art. no. 022317.
[16] I. B. Djordjevic, *Advanced Optical and Wireless Communications Systems*. Cham, Switzerland: Springer, 2017.
[17] I. Djordjevic, "LDPC-coded MIMO optical communication over the atmospheric turbulence channel using Q-ary pulse-position modulation," *Opt. Express*, vol. 15, no. 16, pp. 10026–10032, Aug. 2007.
[18] G. Ungerboeck, "Channel coding with multilevel/phase signals," *IEEE Trans. Inf. Theory*, vol. IT-28, no. 1, pp. 55–67, Jan. 1982.
[19] T. Liu and I. B. Djordjevic, "On the optimum signal constellation design for high-speed optical transport networks," *Opt. Express*, vol. 20, no. 18, pp. 20396–20406, Aug. 2012.

IVAN B. DJORDJEVIC held appointments with the University of the West of England and the University of Bristol, U.K., Tyco Telecommunications, USA, National Technical University of Athens, Greece, and State Telecommunication Company, Yugoslavia. He is currently a Professor in electrical and computer engineering and optical sciences with the University of Arizona, a Director of the Optical Communications Systems Laboratory (OCSL) and Quantum Communications (QuCom) Laboratory, and a Co-Director of the Signal Processing and Coding Laboratory. He has authored or coauthored six books and more than 500 journal and conference publications, and holds 46 U.S. patents.

Mr. Djordjevic serves as a Senior Editor/Member of the Editorial Board for the following journals, IOP *Journal of Optics*, the IEEE COMMUNICATIONS LETTERS, *Physical Communication Journal* (Elsevier), and *Frequenz*. He is an OSA Fellow.